Accessibility of Targeted DHPR Sites to Streptavidin and Functional Effects of Binding on EC Coupling

Nancy M. Lorenzon and Kurt G. Beam

Department of Physiology and Biophysics, University of Colorado Health Sciences Center, Aurora, CO 80045

In skeletal muscle, the dihydropyridine receptor (DHPR) in the plasma membrane (PM) serves as a Ca^{2+} channel and as the voltage sensor for excitation–contraction (EC coupling), triggering Ca^{2+} release via the type 1 ryanodine receptor (RyR1) in the sarcoplasmic reticulum (SR) membrane. In addition to being functionally linked, these two proteins are also structurally linked to one another, but the identity of these links remains unknown. As an approach to address this issue, we have expressed DHPR α_{1S} or β_{1a} subunits, with a biotin acceptor domain fused to targeted sites, in myotubes null for the corresponding, endogenous DHPR subunit. After saponin permeabilization, the ~60-kD streptavidin molecule had access to the β_{1a} N and C termini and to the α_{1S} N terminus and proximal II–III loop (residues 671–686). Steptavidin also had access to these sites after injection into living myotubes. However, sites of the α_{1S} C terminus were either inaccessible or conditionally accessible in saponin-permeabilized myotubes, suggesting that these C-terminal regions may exist in conformations that are occluded by other proteins in PM/SR junction (e.g., RyR1). The binding of injected streptavidin to the β_{1a} N or C terminus, or to the α_{1S} N terminus, had no effect on electrically evoked contractions. By contrast, binding of streptavidin to the proximal α_{1S} II–III loop abolished such contractions, without affecting agonist-induced Ca^{2+} release via RyR1. Moreover, the block of EC coupling did not appear to result from global distortion of the DHPR and supports the hypothesis that conformational changes of the α_{1S} II–III loop are necessary for EC coupling in skeletal muscle.

The Journal of General Physiology

INTRODUCTION

In skeletal muscle, bidirectional signaling occurs between the dihydropyridine receptor (DHPR; a voltage-gated calcium channel composed of a pore-forming α_{1S} subunit and auxiliary subunits α_2-δ, β_{1a}, and γ), and the ryanodine receptor (RyR1; a calcium release channel). Depolarization of the plasma membrane, where DHPRs are located, causes transmission of an orthograde signal from the DHPRs to the RyRs in the SR, resulting in calcium release (Rios and Brum, 1987; Tanabe et al., 1987; Garcia et al., 1994; Dirksen and Beam, 1999). This orthograde, excitation–contraction (EC) coupling signal is independent of the entry of extracellular calcium. In addition, retrograde signaling exists whereby the association with RyR1 increases the magnitude of the voltage-gated Ca^{2+} current carried per DHPR (Nakai et al., 1996).

In addition to functional coupling of the DHPR and RyR1, structural coupling of these two proteins has been suggested from freeze-fracture studies of the plasma membrane, which reveal that DHPRs occur in "tetrads," groups of four intramembranous particles that are arranged in ordered arrays (Franzini-Armstrong and Kish, 1995; Beam and Franzini-Armstrong, 1997; Protasi, 2002). The individual DHPRs within a tetrad are located in exact correspondence to the four subunits of RyR1 (Franzini-Armstrong and Kish, 1995; Block et al., 1988). The arrangement of DHPRs into tetrads is dependent on the presence of RyR1 (Protasi et al., 1998, 2000), implying that the DHPR and RyR1 are linked.

To understand skeletal-type EC coupling it is essential (a) to identify the regions of the DHPR that link it, directly or indirectly, to RyR1, and (b) to establish which of these regions may undergo voltage-driven conformational changes that are necessary for propagating the EC coupling signal. Toward this end, one approach has been to study cDNAs expressed in myotubes. Such approaches have shown that the α_{1S} II–III loop critical domain (Nakai et al., 1998; Kugler et al., 2004) and the β_{1a} C terminus are important for skeletal-type EC coupling (Beurg et al., 1999; Ahern et al., 2001; Sheridan et al., 2003), and that the α_{1S} C terminus is important for targeting DHPRs to plasma membrane/SR junctions (Flucher et al., 2000b; Proenza et al., 2000). Additionally, in vitro biochemical studies have revealed that RyR1 has the ability to bind fragments of the α_{1S} II–III loop and C terminus (Proenza et al., 2002), as well as the β_{1a} C terminus (Cheng et al., 2005). However, considerable uncertainty remains as to whether these binding interactions also occur in vivo. Moreover, none of the studies to date have been able to distinguish whether the identified regions are involved in

Correspondence to Kurt G. Beam: kurt.beam@uchsc.edu

Abbreviations used in this paper: BAD, biotin acceptor domain; 4-CMC, 4-chloro-m-cresol; DHPR, 1,4 dihydropyridine receptor; EC, excitation–contraction; FRET, fluorescence resonance energy transfer; RyR, ryanodine receptor; SA, streptavidin.

static interactions or undergo dynamic rearrangements during EC coupling.

As a new approach, we have begun to use cDNA constructs encoding a consensus sequence for metabolic biotinylation fused to sites of the DHPR. Previously, we employed this approach to demonstrate that after fixation and Triton permeabilization of myotubes expressing these constructs, the ~60-kD molecule streptavidin has access to many sites of DHPRs that are inserted into fully assembled, plasma membrane/SR junctions, but that α_{1S} C-terminal regions may be occluded by RyR1 (Lorenzon et al. 2004).

The goal of the present work was to extend these studies to nonfixed myotubes, both to determine the pattern of streptavidin accessibility under conditions closer to those in vivo and to determine whether the binding of streptavidin interferes with the function of the DHPR as calcium channel and voltage sensor for EC coupling. We have found that in nonfixed, saponin-permeabilized cells, streptavidin has access to all those DHPR sites previously found to be accessible in fixed cells. However, α_{1S} C-terminal sites display a pattern of increased accessibility in nonfixed cells, suggesting that the C terminus exists in at least two conformations, one of which is closely apposed to RyR1. When injected into living myotubes, streptavidin was able to bind to the N and C termini of β_{1a} and to the N terminus of α_{1S}, but this binding did not affect electrically evoked contractions. By contrast, electrically evoked contractions were abolished when injected streptavidin bound to the proximal portion of the α_{1S} II–III loop, consistent with a model in which depolarization causes a rearrangement of the II–III loop such that the critical domain activates RyR1. These data represent the most direct evidence to date that a conformational change of the α_{1S} II–III loop is important for EC coupling.

MATERIALS AND METHODS

cDNA Constructs

The experiments described here made use of cDNA constructs (Fig. 1) that contained sequence for a biotin acceptor domain (BAD) of either 70 or 97 amino acids. The BAD sequence was excised from the PinPoint Xa-1 expression vector (Promega), which encodes a domain of a transcarboxylase subunit from *Propionibacterium shermanii* (PSTCD; PDB code 1DCZ; Reddy et al., 2000). A previous publication (Lorenzon et al., 2004) described the construction of the expression plasmids for YFP-β_{1a}-BAD, BAD-β_{1a}-YFP, BAD-α_{1S}-YFP, α_{1S}(671-BAD-686)-YFP (previously designated α_{1S}(I-II)-BAD-(III-IV)-YFP), YFP-α_{1S}1667-BAD (previously designated YFP-α_{1S}*short*-BAD), and YFP-α_{1S}1860-BAD (previously designated YFP-α_{1S}*long*-BAD). We also analyzed YFP-α_{1S}(1667-BAD)1860, in which the BAD was inserted between α_{1S} C-terminal residue 1667 and the downstream α_{1S} residues 1668–1860. To make this cDNA plasmid, PCR was used to introduce KpnI sites at the start and end of the 70-aa BAD from the PinPoint Xa-1 vector (forward primer GGGGTACCGAGGGCGAGATTCCCGCTC; reverse primer CCGGTACCCGATCTTGATGAGACCCTGACC). A separate PCR reaction was used to remove a KpnI restriction site at the distal α_{1S} C terminus (residue 1860) and introduce a new KpnI site after residue 1667 (forward primer GCCAATGCCAAGGTACCTATGGCAACAGCAGCAACCATAG; reverse primer ATCCCGGGCCCGCGCTACCGTCGACTGGTCA). The plasmids were cut with KpnI, and then the appropriate plasmid fragments were ligated to produce YFP-α_{1S}(1667-BAD)1860. Restriction digests and sequencing were used to verify the construct.

Expression of cDNA

Primary cultures of myotubes isolated from newborn dysgenic (α_{1S}-null) or β_1-null mice were prepared as described previously (Beam and Franzini-Armstrong, 1997). Myoblasts were plated on ECL-coated (Upstate Biotechnology) glass-bottom (MatTek), or primaria plastic (BD Biosciences) 35-mm culture dishes. Myotubes were grown for 6–7 d in a humidified 37°C incubator with 5% CO_2. Approximately 1 wk after plating, myotubes were microinjected (Tanabe et al., 1988) in a single nucleus with a cDNA construct (5–100 ng/μl). After injection, the cells were changed into a medium in which the biotin present in the 2% horse serum was supplemented with an additional 1 μM biotin.

NeutrAvidin Staining and Imaging

2 d after injection, myotubes were washed with an "internal" solution containing (in mM) 140 Cs-aspartate, 10 Cs_2-EGTA, 5 $MgCl_2$, and 10 HEPES, pH to 7.4 with CsOH. The myotubes were permeabilized with saponin (12 μg/ml in internal solution) for 30 s, and then exposed for 30 min in the dark to a 1:2,000 dilution (in internal solution) of NeutrAvidin-tetramethylrhodamine (Molecular Probes), hereafter referred to as "streptavidin." The cells were washed twice with internal solution, fixed with 4% paraformaldehyde in PBS for 20 min, and then imaged with an Axiovert/LSM 510 META laser-scanning confocal microscope (Carl Zeiss MicroImaging, Inc.). Excitation/emission parameters for each fluorophore were as follows: YFP, 488 nm excitation, 488/543 nm dual dichroic, 505–530 nm band-pass emission filter; rhodamine, 543 nm excitation, 488/543 nm dual dichroic, 560 nm long-pass emission filter. Cells were viewed with 40× (1.3 NA) or 63× (1.4 NA) oil immersion objectives.

Evoked Contractions and Streptavidin Injection

Myotubes were bathed in a rodent Ringers solution containing (in mM) 146 NaCl, 5 KCl, 2 CaCl, 1 MgCl2, 10 HEPES, 11 glucose (pH to 7.4 with NaOH) and tested for electrically evoked contractions (extracellular stimulation 100 V, 10–20 ms). Cells that produced robust contractions were then bathed in Ringers solution containing *N*-benzyl-*p*-toluene sulphonamide (BTS; 10 μm) for 5–10 min to block contractions during subsequent microinjection with streptavidin (1 mg/ml). The cells were rinsed twice with culture medium and returned to the tissue culture incubator for at least 2 h. The identified myotubes were then retested for evoked contractions under the same conditions as before streptavidin injection. Records of contractions were obtained by measuring the movement of an identifiable portion of a myotube across the visual field from confocal images acquired at a rate of 11 Hz.

Calcium Transients and Streptavidin Injection

To analyze intracellular Ca^{2+} transients in response to membrane depolarization or to direct ryanodine receptor activation, intact myotubes were loaded with the fluorescent calcium indicator dye Fluo-3 AM. Before imaging, myotubes were washed free of the culture medium with rodent Ringer and exposed to the dye (5 μM in rodent Ringer) for 1 h at 37°C. Calcium transients were recorded in response to membrane depolarization by 80 mM KCl or RyR1 activation by 0.5 mM 4-chloro-m-cresol (4-CmC), which were applied for 5 s via an extracellular pipette. Calcium transients were measured as a change in fluorescence

intensity (ΔF/F) using confocal imaging (excitation/emission parameters for fluo3-AM dye: 488 nm excitation, 505 nm LP emission filter).

Whole-Cell Recording Methods

Calcium currents were recorded with the whole-cell variant of the patch clamp technique. Pipettes were fabricated from borosilicate glass and had resistances of 1.5–2.4 MΩ when filled with internal solution (composition given above). For the measurement of membrane currents, the external solution contained (in mM): 145 tetraethylammonium-Cl, 10 $CaCl_2$, 10 HEPES, and 0.003 tetrodotoxin, pH 7.4 with tetraethylammonium-OH. Test currents were corrected for linear components of leak and capacitative currents by digital scaling and subtraction of averaged control currents elicited by 20-mV hyperpolarizing steps from the holding potential (−80 mV). Cell capacitance was determined by integration of these same control currents and used to normalize test currents (pA/pF). To inactivate T-type currents and isolate L-type currents, a 1-s prepulse to −30 mV followed by a 100-ms repolarization to −50 mV was applied before the test pulse.

RESULTS

Fig. 1 illustrates the constructs used, all of which contained BAD at one site and fluorescent protein at a second site as an independent reporter of DHPR localization. Except for YFP-α_{1S}(1667-BAD)1860, these constructs were examined in a previous study (Lorenzon et al., 2004) and found able to restore electrically evoked contractions. We also found this to be the case for YFP-α_{1S}(1667-BAD)1860 expressed in α_{1S}-null myotubes (12/13 cells). Thus, the incorporation of a BAD did not appear to interfere with the targeting or essential function of the α_{1S} or β_{1a} fusion proteins.

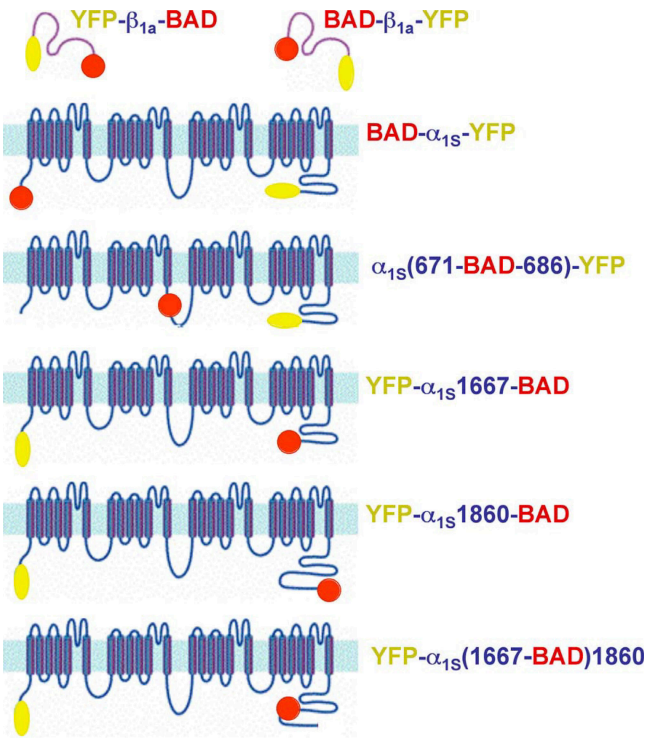

Figure 1. Schematic illustration of the BAD-DHPR fusion constructs. Constructs are designated by the sites of attachment of BAD (red circle) and YFP (yellow oval). In the α_{1S} II–III loop constructs, α_{1S} residues 672–685 were replaced by the BAD. For the α_{1S} C terminus, BAD was attached after residue 1860, or attached after residue 1667, or placed after 1667 followed by α_{1S} 1668–1860 (YFP-α_{1S}(1667-BAD)1860).

Streptavidin Accessibility of Targeted DHPR Sites

Our previous work (Lorenzon et al. 2004) showed that in fixed and Triton-permeabilized myotubes, streptavidin had access to all of the sites illustrated in Fig. 1, except for BAD fused to the end of either the proximal (YFP-α_{1S}1667-BAD) or distal (YFP-α_{1S}1860-BAD) C terminus. Both of these sites were occluded in the presence of RyR1. An important goal of the present studies was to assay streptavidin accessibility under conditions similar to those in vivo. As one part of this effort,

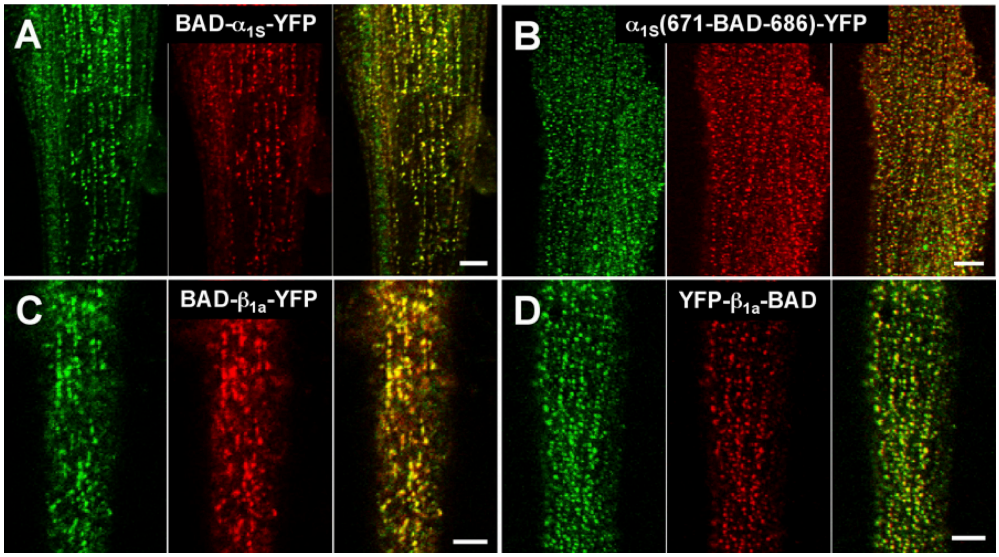

Figure 2. In nonfixed myotubes, the α_{1S} N terminus, the α_{1S} proximal II–III loop, and the N and C terminus of β_{1a} are accessible to streptavidin (A–D, respectively). Left panels illustrate the localization of the YFP-DHPR fusion proteins (indicated in green), center panels illustrate the localization of the bound streptavidin (red), and right panels show the overlay. Bars, 5 μm.

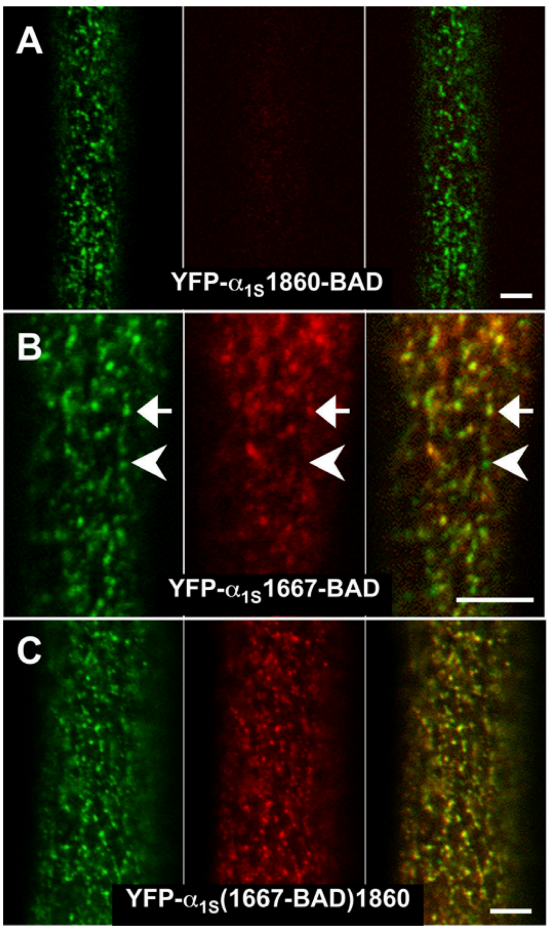

Figure 3. Differential accessibility of α_{1S} C-terminal sites to streptavidin in nonfixed myotubes. (A) Myotubes expressing YFP-α_{1S}1860-BAD did not display binding of streptavidin that colocalized with loci of fluorescent DHPRs. (B) Myotubes expressing YFP-α_{1S}1667-BAD displayed incomplete colocalization between loci of DHPRs and streptavidin binding. The arrow indicates a cluster of DHPRs with substantial binding of streptavidin, and the arrowhead a cluster of DHPRS showing very little binding of streptavidin. (C) Nearly complete colocalization was observed for YFP-α_{1S}(1667-BAD)1860. Bars, 5 μm.

nonfixed cells expressing the DHPR-BAD fusion proteins were saponin permeabilized, and then exposed to streptavidin. Saponin-permeabilized myotubes retain substantial function as shown by both spontaneous Ca^{2+} release and caffeine-induced global Ca^{2+} release (Ward et al., 2000, 2001).

As in fixed myotubes, BAD fused to the α_{1S} N terminus was accessible in nonfixed myotubes to the ~60-kD streptavidin molecule (Fig. 2 A). Specifically, red fluorescent foci (center panel), representing bound streptavidin, were colocalized with the foci of fluorescent protein (indicated in green, left), which report the distribution of the α_{1S} subunit. BAD inserted into the proximal region of the α_{1S} II–III loop (replacing α_{1S} residues 671–686) was also accessible to streptavidin binding (Fig. 2 B) in nonfixed myotubes. A similar pattern of

TABLE I

Streptavidin Colocalization and Accessibility to Various DHPR Sites in Nonfixed Myotubes

DHPR/BAD construct	# cells exhibiting colocalization	Colocalization score
BAD-β_{1a}-YFP	12 (12)	1.9 (11)
YFP-β_{1a}-BAD	16 (16)	1.8 (11)
BAD-α_{1S}-YFP	13 (13)	1.8 (7)
α_{1S}(671-BAD-686)-YFP	12 (12)	1.7 (10)
YFP-α_{1S}1860-BAD	1[a] (23)	0.1 (12)
YFP-α_{1S}1667-BAD	30[a] (39)	0.8 (17)
YFP-α_{1S}(1667-BAD)1860	21 (21)	1.9 (12)

The total number of cells examined for each construct noted in parentheses. [a]The YFP-α_{1S}1860-BAD and YFP-α_{1S}1667-BAD cells exhibited partial colocalization (considerably fewer dots were colocalized compared to the other constructs).

colocalizing red and green foci was present for the N and C termini of the β_{1a} subunit (Fig. 2, C and D). Thus, the accessibility of all these sites to streptavidin was similar in fixed and nonfixed myotubes.

The only DHPR site that showed a difference in streptavidin accessibility in nonfixed versus fixed myotubes was the proximal portion of the α_{1S} C terminus. In fixed dysgenic myotubes (Lorenzon et al., 2004), both the distal α_{1S} C terminus (YFP-α_{1S}1860-BAD) and proximal, truncated α_{1S} C terminus (YFP-α_{1S}1667-BAD) were inaccessible to streptavidin. In nonfixed cells, the distal α_{1S} C terminus (YFP-α_{1S}1860-BAD) was also inaccessible. The lack of accessibility is illustrated in Fig. 3 A, where YFP-α_{1S}1860-BAD and streptavidin puncta did not colocalize (especially apparent in the overlay image, right). However, in distinction to fixed myotubes, the proximal, truncated α_{1S} C terminus (YFP-α_{1S}1667-BAD) was at least partially accessible in nonfixed myotubes (see both the presence and absence of streptavidin puncta colocalized with the YFP puncta in Fig. 3 B). To investigate this partial accessibility further, we examined streptavidin binding to BAD inserted at the identical, proximal position, but followed by the additional, C-terminal sequence, YFP-α_{1S}(1667-BAD)1860. The presence of this additional C-terminal sequence caused BAD at residue 1667 to be accessible to streptavidin in nonfixed myotubes (Fig. 3 C).

Table I summarizes the extent of colocalization between streptavidin binding and clusters of DHPRs. The first data column presents the judgment of the authors, based on identified images. The majority of these same images were also randomly assembled and presented unidentified to four individuals who assigned each image a numerical value of 0 (<5% colocalization), 1 (5–95% colocalization), or 2 (>95% colocalization). The mean values for these scores are presented in Table I, data column 2, and agree well with the authors' assessment of identified images.

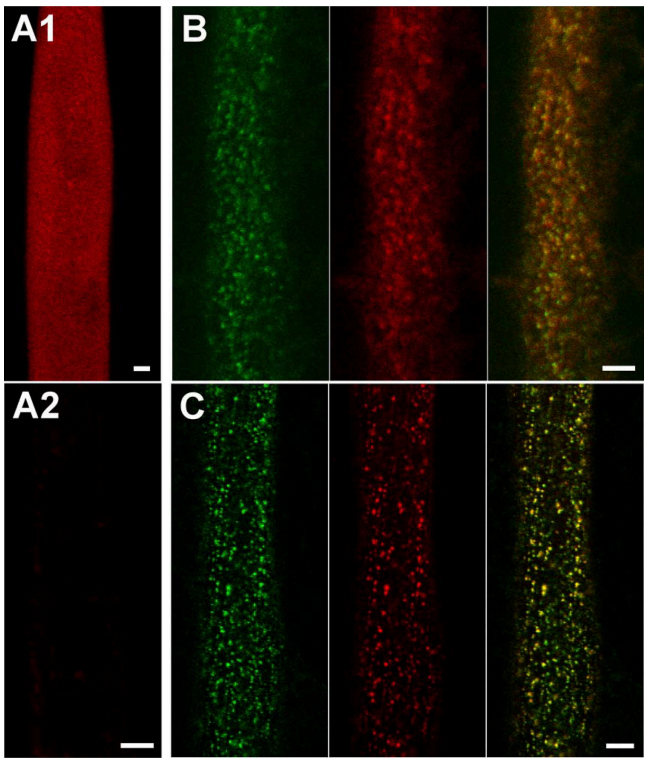

Figure 4. Diffusion and binding of streptavidin injected into living myotubes. (A1) 1 h after streptavidin (SA) injection of a normal myotube, diffuse red fluorescence could be observed throughout the cell. (A2) In the absence of DHPR-BAD fusion proteins, injected streptavidin is rapidly released after saponin permeabilization. 1 h after SA injection of a normal myotube, saponin was applied and an image obtained ~15 min later with laser intensity, detector/amplifier gains, and offset set to be the same as for the images in B. (B) A 1-h period was sufficient to allow binding of injected streptavidin to BAD-α_{1S}-YFP expressed in a dysgenic myotube. Nonbound streptavidin was released by saponin permeabilization. Bars, 5 μm. (C) Colocalization of red and yellow fluorescent puncta from injected streptavidin-rhodamine and YFP-β_{1a}-BAD in a β_1-null myotube. Note that BAD-β_{1a}-YFP streptavidin binding has not yet been confirmed by confocal imaging.

Functional Impact of Streptavidin Binding

The ability of streptavidin to bind at DHPR sites in nonfixed myotubes raises the question of whether the addition of this large mass interferes with the function of the DHPR as the voltage sensor for EC coupling. To address this question, saponin permeabilization was not an appropriate method of applying streptavidin, which was introduced instead by intracellular microinjection. For this approach, it was important to determine (a) whether injected streptavidin could diffuse and bind to DHPR sites within intact myotubes, and (b) whether injected streptavidin interferes with the function of normal myotubes. Fig. 4 A1 demonstrates that injected streptavidin (1 mg/ml) uniformly filled a large myotube within 1 h after injection. To determine if this period of time was also sufficient for binding, it was necessary first to release unbound streptavidin from the cell, which was accomplished by saponin permeabilization. Fig. 4 A2 shows for a normal myotube (which lacks DHPR-BAD fusion protein) that virtually no unbound streptavidin remains following this permeabilization. Fig. 4 (B and C) illustrates myotubes expressing either BAD-α_{1S}-YFP or YFP-β_{1a}-BAD, which were injected with streptavidin and 1 h later subjected to saponin permeabilization. The colocalization of red and green foci indicates that streptavidin binding had occurred during the previous 1-h incubation. As a final control experiment, normal myotubes were tested for EC coupling 2–5 h after injection of streptavidin. Extracellular stimulation of such myotubes elicited brief, strong contractions (29/29 cells; unpublished data).

To test the effects of streptavidin binding on EC coupling, individual dysgenic or β_1-null myotubes expressing DHPR/BAD fusion constructs were initially tested for electrically evoked contractions before streptavidin injection (Fig. 5, top). At least 2 h after injection, the identified cells were retested for evoked contractions (Fig. 5, bottom). Evoked contractions were not affected by streptavidin binding to the N or C terminus of β_{1a} (10/11 and 18/20 cells contracted, respectively) or to the α_{1S} N terminus (10/11 cells). However, binding of streptavidin to the proximal portion of the α_{1S} II–III loop abolished evoked contractions (Fig. 5, weak contraction in 1/12 cells; no contractions in the remainder). Thus, the II–III loop was the only DHPR site at which the additional mass of streptavidin interfered with EC coupling.

Electrically evoked contractions require that a brief depolarization produce substantial Ca^{2+} release. Thus, a partial reduction of Ca^{2+} release might account for the loss of electrically evoked contractions after streptavidin binding to the proximal II–III loop. To test this, we examined Ca^{2+} release in response to a more prolonged depolarization produced by application of 80 mM KCl. Fig. 6 (top) shows that Ca^{2+} released by a 5-s depolarization was reduced to a nearly undetectable level by streptavidin binding to the proximal II–III loop. This nearly complete suppression of EC coupling was not a consequence of depletion of SR Ca^{2+} stores or a direct effect of streptavidin on RyR1. Specifically, Fig. 6 (bottom) shows that Ca^{2+} release in response to the RyR agonist, 4-CmC, was not obviously different in streptavidin-injected, α_{1S}(671-BAD-686)-YFP–expressing myotubes.

In principle, the binding of streptavidin to the α_{1S} II–III loop could have prevented a specific conformational change necessary for EC coupling without affecting other functions of the DHPR. Alternatively, this binding could have induced a widespread distortion of α_{1S} that abolished function of the DHPR more globally. Fig. 7 illustrates calcium currents in myotubes expressing α_{1S}(671-BAD-686)-YFP that were injected

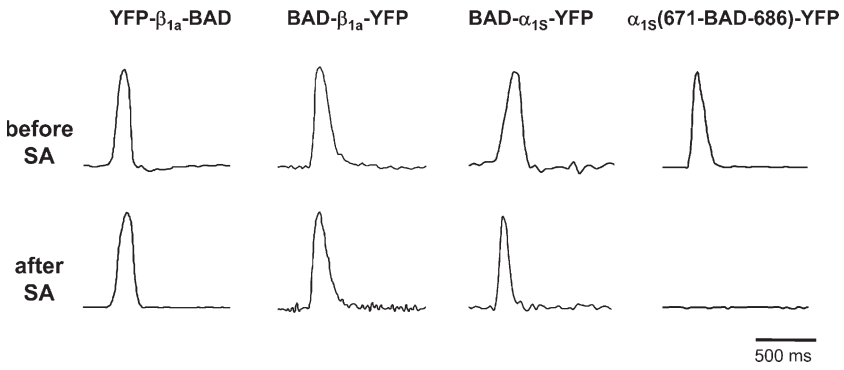

Figure 5. Excitation-contraction coupling is abolished by streptavidin binding to the proximal portion of the α_{1S} II-III loop, but is unaffected when binding occurs at the α_{1S} N terminus or β_{1a} N or C terminus. Electrically evoked contractions are shown for intact β_1-null myotubes expressing YFP-β_{1a}-BAD or BAD-β_{1a}-YFP, or dysgenic myotubes expressing BAD-α_{1S}-YFP or α_{1S}(671-BAD-686)-YFP. Prior to streptavidin injection, myotubes responded to extracellular stimulation with robust contractions (top). 2–4 h after streptavidin injection, the same individual myotubes were tested for their responses to identical stimulation (bottom). Vertical scale, arbitrary units. For BAD-β_{1a}-YFP–expressing cells, streptavidin binding following injection has not yet been confirmed by confocal imaging.

with streptavidin. Streptavidin had no obvious effect on either the voltage dependence or amplitude of Ca^{2+} currents in these cells. The average peak amplitude of currents in α_{1S}(671-BAD-686)-YFP–expressing cells was similar whether or not streptavidin was injected (Fig. 7 B) and comparable to that of dysgenic myotubes expressing α_{1S}-YFP (Bannister and Beam, 2005). Thus, the ability of α_{1S}(671-BAD-686)-YFP to function in EC coupling was eliminated by streptavidin binding, whereas its function as a calcium channel and its retrograde regulation from RyR1 were not affected. Although not systematically examined, we also found no obvious effect of injected streptavidin on Ca^{2+} currents in myotubes expressing YFP-β_{1a}-BAD, BAD-β_{1a}-YFP, or BAD-α_{1S}-YFP (unpublished data).

DISCUSSION

In this paper, we have examined the consequences of applying streptavidin to myotubes expressing DHPRs with targeted sites of biotinylation. Except for the α_{1S} C terminus, all other DHPR sites examined, including the α_{1S} N terminus and proximal II–III loop and the β_{1a} N and C termini, were accessible to streptavidin binding and showed equivalent accessibility in nonfixed myotubes as found previously (Lorenzon et al., 2004) for fixed cells. However, the accessibility of the α_{1S} C terminus differed between fixed and nonfixed cells and depended on the location of the BAD, the length of the C terminus, and the presence or absence of RyR1. In addition to examining accessibility, we also characterized the functional consequences of streptavidin binding at sites of the α_{1S} and β_{1a} subunits. Excitation–contraction coupling was abolished by streptavidin binding to the proximal portion of the α_{1S} II–III loop, but was unaffected by binding at the α_{1S} N terminus or β_{1a} N or C terminus.

Streptavidin Accessibility

Except for the α_{1S} C terminus, all other sites of α_{1S} and β_{1a} showed equivalent accessibility in fixed and nonfixed cells. The ability of streptavidin to bind to the C terminus appears to depend on the location of the BAD within the C terminus, the length of the C terminus,

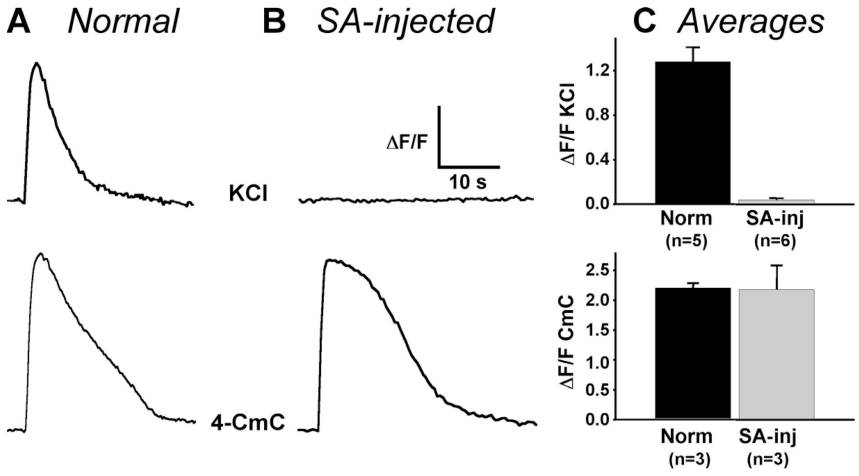

Figure 6. Effect of streptavidin binding to the proximal α_{1S} II–III loop on depolarization- and 4-CmC–induced Ca^{2+} transients. Representative responses are shown for normal myotubes (A) and SA-injected α_{1S}(671-BAD-686)-YFP–expressing myotubes (B) to a 5-s application of either 80 mM KCl (top) or 0.5 mM 4-CmC (bottom). ΔF/F scale bar = 0.4 or 0.6 for the KCl responses of the normal and SA-injected myotubes, respectively, and 1.0 or 0.6 for the 4-CmC responses of the normal and SA-injected myotubes, respectively. (C) Summary of peak ΔF/F amplitudes for KCl (top) and 4-CmC (bottom) responses of either normal myotubes (Norm) or SA-injected α_{1S}(671-BAD-686)-YFP–expressing myotubes (SA-inj).

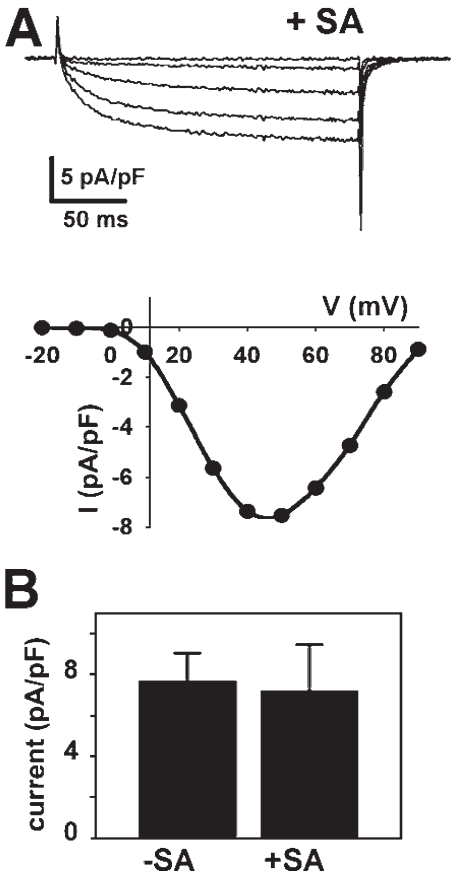

Figure 7. Streptavidin binding to the proximal portion of the α_{1S} II–III loop has little effect on calcium currents. (A) Currents were recorded from a dysgenic myotube expressing α_{1S}(671-BAD-686)-YFP that was injected with streptavidin-rhodamine >2 h before recording. The plot shows the I-V relationship for α_{1S}(671-BAD-686)-YFP currents following streptavidin injection. (B) The average amplitudes of calcium currents evoked by a 200-ms voltage step to +40 mV from α_{1S}(671-BAD-686)-YFP–expressing myotubes that were not (−SA, n = 4 cells) or were (+SA, n = 8 cells) injected with streptavidin.

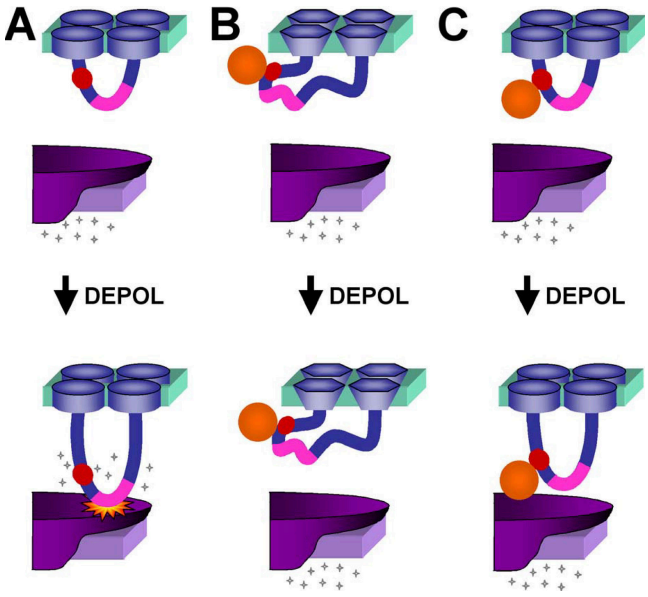

Figure 8. Possible mechanisms for how binding of streptavidin to the α_{1S} II-III loop could interfere with EC coupling. (A) During normal EC coupling, membrane depolarization induces a conformational change in the α_{1S} II–III loop, which causes the activation of RyR1 (indicated by "starburst") and release of calcium. The inserted BAD (red circle) is proximal to the "critical domain" (pink) and does not interfere with these events. (B) Binding of streptavidin could globally distort α_{1S} such that the channel protein becomes nonfunctional. This possibility appears to be excluded since streptavidin binding did not affect the amplitude or gross voltage dependence of calcium currents. (C) Binding of streptavidin could interfere with the RyR1-activating conformational change of the II–III loop or another cytoplasmic portion of the DHPR.

and the presence of RyR1. The distal C terminus (residue 1860) is not accessible in either fixed or nonfixed cells, suggesting that this region may be buried. However, the accessibility of the proximal C terminus (residue 1667) is more complex. The BAD is partially accessible when attached at the end of a truncated (after residue 1667) C terminus in nonfixed myotubes (Fig. 3 B), but inaccessible in fixed myotubes (Lorenzon et al., 2004). Our data do not allow us to differentiate between the possibilities that the proximal α_{1S} C terminus is partially accessible in all junctions or ranges from accessible to inaccessible, perhaps as a consequence of developmental maturity of the junctions. In either case, it is necessary to suppose that fixation reduces the partial accessibility of the proximal α_{1S} C terminus to below the level of detection.

The partial accessibility of the proximal α_{1S} C terminus in nonfixed myotubes could also reflect the existence of two, functionally distinct conformations, one of which is occluded by RyR1 and one which is not. If the fractional occupancy of the nonoccluded state was only a few percent, nearly all sites would be occluded after fixation. Furthermore, the binding of streptavidin in nonfixed cells would gradually trap the proximal C terminus in the nonoccluded conformation, resulting in partial colocalization of streptavidin with junctional DHPRs. However, BAD attached at the identical, proximal site (1667) within a longer C terminus (BAD followed by α_{1S} residues 1668–1860) was accessible to streptavidin in nonfixed myotubes (Fig. 3 C), suggesting that the distal C terminus may anchor the proximal C terminus in a nonoccluded conformation.

The pattern of streptavidin accessibility to DHPR sites is in good agreement with a previous study using the complementary approach of measuring the fluorescence resonance energy transfer (FRET) efficiency of a CFP-YFP tandem attached to these same sites of DHPRs within junctions that either did, or did not, contain RyR1 (Papadopoulos et al., 2004). In that FRET study, a difference in FRET was taken as an indication that the presence of RyR1 impacted the environment of the attachment site. In agreement with the present work, the

FRET efficiency was equivalent in the presence and absence of RyR1 when the reporter was attached to the α_{1S} N terminus and proximal II–III loop, and to the β_{1a} C terminus. The two methods were also in quite good agreement for the α_{1S} C terminus truncated at 1667, where the presence of RyR1 resulted in incomplete accessibility to streptavidin and reduced CFP-YFP FRET. The β_{1a} N terminus was the only site for which the two methods gave different results in that the presence of RyR1 did not prevent streptavidin accessibility but did alter CFP-YFP FRET. One could imagine that the β_{1a} N terminus is close to RyR1 but that biotin projects from the attached BAD in an orientation that allows streptavidin accessibility.

The proximal C-terminal site examined in our studies (residue 1667) lies near the site at which naturally occurring, proteolytic cleavage has been reported to cause truncation of ~95% of α_{1S} in adult skeletal muscle (De Jongh et al., 1991; Hulme et al., 2005). With respect to the distal site (residue 1860) examined in the present study, it is important to note that a much larger fraction (~30%) of α_{1S} in cultured myotubes is full length (Shulman, 1996). Moreover, Catterall and colleagues (Hulme et al., 2005) propose that the A-kinase anchoring protein, AKAP15, anchors the cleaved portion of the C terminus to the proximal portion. In any case, there is good evidence that a large fraction of α_{1S} in myotubes has the distal C terminus attached (Flucher et al., 2000a), although the nature of this attachment remains unclear.

A number of possible roles have been ascribed to the C-terminal tails of L-type Ca^{2+} channels. In particular, portions of the C terminus of α_{1C} (Gao et al., 2000) and α_{1S} (Proenza et al., 2000) may be important both for trafficking to the plasma membrane, and for targeting to plasma membrane junctions with the SR (Flucher et al., 2000b; Proenza et al., 2000). Moreover, biochemical studies have suggested that the C-terminal residues 1393–1527 of α_{1S} bind calmodulin and can bind to RyR1 (Sencer et al., 2001). Additionally, both the α_{1S} C terminus (residues 1431–1435) and RyR1 contain consensus binding sites for Homer (Xiao et al., 2000). Perhaps the direct or indirect linkage of α_{1S} C-terminal residues to RyR1 has the consequence that the distal C terminus of α_{1S} is inaccessible to streptavidin in RyR1-containing junctions, either because RyR1 directly occludes the distal C terminus or because the RyR1-induced arrangement of DHPRs into tetrads results in occlusion.

Functional Impact of Streptavidin Binding: Direct Evidence that EC Coupling Depends on a Conformational Change Involving the α_{1S} II–III Loop

Previous work has implicated a variety of DHPR sites as important for EC coupling, including the II–III loop critical domain and the III–IV loop of α_{1S} and the C terminus of the β_{1a}. In particular, studies using expression in myotubes null for α_{1S} or β_{1a} have shown that mutations and/or deletions within the aforementioned regions profoundly affect EC coupling (Nakai et al., 1998; Beurg et al., 1999; Ahern et al., 2001; Sheridan et al., 2003; Kugler et al., 2004). A priori, these regions could be directly involved in protein–protein interactions linking DHPRs to RyRs, but they could equally well impact the ability of other regions of the DHPR to participate in such interactions. Additionally, current candidate regions of the DHPR could either be involved in static interactions that link DHPRs to RyRs, or actively undergo conformational changes that are essential for propagating the EC coupling signal. Unfortunately, the functional analyses to date do not provide a basis for distinguishing these possibilities.

Here we have found that excitation–contraction coupling is abolished by streptavidin binding to the proximal portion of the α_{1S} II–III loop, but is unaffected when binding occurs at the α_{1S} N terminus or β_{1a} N or C terminus. Fig. 8 illustrates a model of EC coupling together with mechanisms by which streptavidin binding could interfere with this coupling. In particular, EC coupling is pictured (Fig. 8 A) as dependent upon a conformational change of the α_{1S} II–III loop with the result that the critical domain (residues 720–765, pink) contacts RyR1 and activates it to release Ca^{2+} from the SR. Conceivably, the binding of streptavidin to the proximal II–III loop could distort the overall structure of the DHPR so as to entirely abolish the function of this protein (Fig. 8 B). This possibility would appear to be excluded by the result that calcium currents are unaffected by the binding of streptavidin to the II–III loop. Importantly, the amplitude of DHPR Ca^{2+} current depends not only on the structural integrity of the DHPR but also on a retrograde functional interaction between RyR1 and the DHPR (Nakai et al., 1996). This retrograde interaction is abolished by structural alterations of the critical domain of the α_{1S} II–III loop (Grabner et al., 1999; Kugler et al., 2004). Thus, the fact that Ca^{2+} current amplitude was unaffected by streptavidin binding to the proximal II–III loop provides additional support that this binding does not significantly distort the spatial interrelationship between the DHPR and RyR1.

As an alternative to a global disruption of structure, bound streptavidin could specifically obstruct conformational changes of DHPR cytoplasmic domains required for EC coupling. As shown in Fig. 8 C, streptavidin bound to the proximal II–III loop interferes with the conformational change that causes the downstream, critical domain to contact RyR1. An alternative possibility is that the critical domain contacts RyR1 at rest and that bound streptavidin prevents a torsional conformational change that is necessary for activation of Ca^{2+} release. In any case, our results provide the most direct evidence to date that conformational changes of the α_{1S} II–III loop are critical for EC coupling, but do not

preclude the possibility of additional, important conformational changes of other DHPR cytoplasmic domains.

We thank Roger Bannister for assistance with the electrophysiology.

This work was supported by National Institutes of Health grant NS24444 (K.G. Beam).

Angus C. Nairn served as editor.

Submitted: 30 December 2006
Accepted: 4 September 2007

REFERENCES

Ahern, C.A., D. Bhattacharya, L. Mortenson, and R. Coronado. 2001. A component of excitation-contraction coupling triggered in the absence of the T671-L690 and L720-Q765 regions of the II-III loop of the dihydropyridine receptor α_{1S} pore subunit. *Biophys. J.* 81:3294–3307.

Bannister, R.A., and K.G. Beam. 2005. The α_{1S} N-terminus is not essential for bi-directional coupling with RyR1. *Biochem. Biophys. Res. Commun.* 336:134–141.

Beam, K.G., and C. Franzini-Armstrong. 1997. Functional and structural approaches to the study of excitation-contraction coupling. *Methods Cell Biol.* 52:283–306.

Beurg, M., C.A. Ahern, P. Vallejo, M.W. Conklin, P.A. Powers, R.G. Gregg, and R. Coronado. 1999. Involvement of the carboxy-terminus region of the dihydropyridine receptor β1a subunit in excitation-contraction coupling of skeletal muscle. *Biophys. J.* 77:2953–2967.

Block, B.A., T. Imagawa, K.P. Campbell, and C. Franzini-Armstrong. 1988. Structural evidence for direct interaction between the molecular components of the transverse tubule/sarcoplasmic reticulum junction in skeletal muscle. *J. Cell Biol.* 107:2587–2600.

Cheng, W., A. Xavier, M. Ronjat, and R. Coronado. 2005. Interaction between the dihydropyridine receptor Ca^{2+} channel β-subunit and ryanodine receptor type 1 strengthens excitation-contraction coupling. *Proc. Natl. Acad. Sci. USA.* 102:19225–19230.

De Jongh, K.S., C. Warner, A.A. Colvin, and W.A. Catterall. 1991. Characterization of the two size forms of the α1 subunit of skeletal muscle L-type calcium channels. *Proc. Natl. Acad. Sci. USA.* 88:10778–10782.

Dirksen, R.T., and K.G. Beam. 1999. Role of calcium permeation in dihydropyridine receptor function. Insights into channel gating and excitation-contraction coupling. *J. Gen. Physiol.* 114:393–403.

Flucher, B.E., N. Kasielke, U. Gerster, B. Neuhuber, and M. Grabner. 2000a. Insertion of the full-length calcium channel α_{1S} subunit into triads of skeletal muscle in vitro. *FEBS Lett.* 474:93–98.

Flucher, B.E., N. Kasielke, and M. Grabner. 2000b. The triad targeting signal of the skeletal muscle calcium channel is localized in the COOH terminus of the α_{1S} subunit. *J. Cell Biol.* 151:467–477.

Franzini-Armstrong, C., and J.W. Kish. 1995. Alternate disposition of tetrads in peripheral couplings of skeletal muscle. *J. Muscle Res. Cell Motil.* 16:319–324.

Gao, T., M. Bunemann, B.L. Gerhardstein, H. Ma, and M.M. Hosey. 2000. Role of the C terminus of the α_{1C} (Cav1.2) subunit in membrane targeting of cardiac L-type calcium channels. *J. Biol. Chem.* 275:25436–25444.

Garcia, J., T. Tanabe, and K.G. Beam. 1994. Relationship of calcium transients to calcium currents and charge movements in myotubes expressing skeletal and cardiac DHP receptors. *J. Gen. Physiol.* 103:125–147.

Grabner, M., R.T. Dirksen, N. Suda, and K.G. Beam. 1999. The II-III loop of the skeletal muscle dihydropyridine receptor is responsible for the bi-directional coupling with the ryanodine receptor. *J. Biol. Chem.* 274:21913–21919.

Hulme, J.T., K. Konoki, T.W.-C. Lin, M.A. Gritsenko, D.G. Camp, D.J. Bigelow, and W.A. Catterall. 2005. Sites of proteolytic processing and noncovalent association of the distal C-terminal domain of Cav1.1 channels in skeletal muscle. *Proc. Natl. Acad. Sci. USA.* 102:5274–5279.

Kugler, G., R.G. Weiss, B.E. Flucher, and M. Grabner. 2004. Structural requirements of the dihydropyridine receptor α1S II-III loop for skeletal-type excitation-contraction coupling. *J. Biol. Chem.* 279:4721–4728.

Lorenzon, N.M., C.S. Haarmann, E.E. Norris, S. Papadopoulos, and K.G. Beam. 2004. Metabolic biotinylation as a probe of supramolecular structure of the triad junction in skeletal muscle. *J. Biol. Chem.* 279:44057–44064.

Nakai, J., R.T. Dirksen, H.T. Nguyen, I.N. Pessah, K.G. Beam, and P.D. Allen. 1996. Enhanced dihydropyridine receptor channel activity in the presence of ryanodine receptor. *Nature.* 380:72–75.

Nakai, J., T. Tanabe, T. Konno, B. Adams, and K.G. Beam. 1998. Localization in the II-III loop of the dihydropyridine receptor of a sequence critical for excitation-contraction coupling. *J. Biol. Chem.* 273:24983–24986.

Papadopoulos, S., V. Leuranger, R. Bannister, and K.G. Beam. 2004. Mapping sites of potential proximity between the dihydropyridine receptor and RyR1 in muscle using a cyan fluorescent protein-yellow fluorescent protein tandem as a fluorescence resonance energy transfer probe. *J. Biol. Chem.* 279:44046–44056.

Proenza, C., C. Wilkens, N.M. Lorenzon, and K.G. Beam. 2000. A carboxyl-terminal region important for the expression and targeting of the skeletal muscle dihydropyridine receptor. *J. Biol. Chem.* 275:23169–23174.

Proenza, C., J.J. O'Brien, J. Nakai, S. Mukherjee, P.D. Allen, and K.G. Beam. 2002. Identification of a region of RyR1 that participates in allosteric coupling with the α_{1S} ($Ca_V1.1$) II-III loop. *J. Biol. Chem.* 277:6530–6535.

Protasi, F. 2002. Structural interaction between RYRs and DHPRs in calcium release units of cardiac and skeletal muscle cells. *Front. Biosci.* 7:D650–D658.

Protasi, F., C. Franzini-Armstrong, and P.D. Allen. 1998. Role of ryanodine receptors in the assembly of calcium release units in skeletal muscle. *J. Cell Biol.* 140:831–842.

Protasi, F., H. Takekura, Y. Wang, S.R. Chen, G. Meissner, P.D. Allen, and C. Franzini-Armstrong. 2000. RYR1 and RYR3 have different roles in the assembly of calcium release units of skeletal muscle. *Biophys. J.* 79:2494–2508.

Reddy, D.V., B.C. Shenoy, P.R. Carey, and F.D. Sonnichsen. 2000. High resolution solution structure of the 1.3S subunit of transcarboylase from *Proprionibacterium shermanii*. *Biochemistry.* 39:2509–2516.

Rios, E., and G. Brum. 1987. Involvement of dihydropyridine receptors in excitation-contraction coupling in skeletal muscle. *Nature.* 325:717–720.

Sencer, S., R.V. Papineni, D.B. Halling, P. Pate, J. Krol, J.Z. Zhang, and S.L. Hamilton. 2001. Coupling of RYR1 and L-type calcium channels via calmodulin binding domains. *J. Biol. Chem.* 276:38237–38241.

Sheridan, D.C., W. Cheng, C.A. Ahern, L. Mortenson, D. Alsammarae, P. Vallejo, and R. Coronado. 2003. Truncation of the carboxyl terminus of the dihydropyridine receptor β1a subunit promotes Ca^{2+} dependent excitation-contraction coupling in skeletal myotubes. *Biophys. J.* 84:220–237.

Shulman, D. 1996. Expression of calcium channel α_1 isoforms in skeletal muscle during in vivo and in vitro development. Ph.D. thesis. Colorado State University, Fort Collins, CO. 82 pp.

Tanabe, T., H. Takeshima, A. Mikami, V. Flockerzi, H. Takahashi, K. Kangawa, M. Kojima, H. Matsuo, T. Hirose, and S. Numa. 1987. Primary structure of the receptor for calcium channel blockers from skeletal muscle. *Nature.* 328:313–318.

Tanabe, T., K.G. Beam, J.A. Powell, and S. Numa. 1988. Restoration of excitation-contraction coupling and slow calcium current in dysgenic muscle by dihydropyridine receptor complementary DNA. *Nature.* 336:134–139.

Ward, C.W., M.F. Schneider, D. Castillo, F. Protasi, Y. Wang, S.R. Chen, and P.D. Allen. 2000. Expression of ryanodine receptor RyR3 produces Ca^{2+} sparks in dyspedic myotubes. *J. Physiol.* 525:91–103.

Ward, C.W., F. Protasi, D. Castillo, Y. Wang, S.R. Chen, I.N. Pessah, P.D. Allen, and M.F. Schneider. 2001. Type 1 and type 3 ryanodine receptors generate different Ca^{2+} release event activity in both intact and permeabilized myotubes. *Biophys. J.* 81:3216–3230.

Xiao, B., J.C. Tu, and P.F. Worley. 2000. Homer: a link between neural activity and glutamate receptor function. *Curr. Opin. Neurobiol.* 10:370–374.